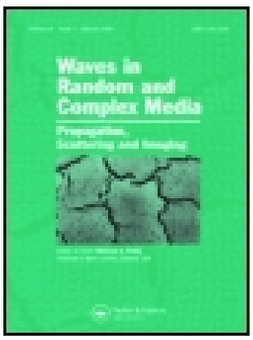

Waves in Random and Complex Media

ISSN: (Print) (Online) Journal homepage: https://www.tandfonline.com/loi/twrm20

A neuronal population model based on cellular automata to simulate the electrical waves of the brain

Ali Khaleghi, Mohammad Reza Mohammadi, Kian Shahi & Ali Motie Nasrabadi

To cite this article: Ali Khaleghi, Mohammad Reza Mohammadi, Kian Shahi & Ali Motie Nasrabadi (2021): A neuronal population model based on cellular automata to simulate the electrical waves of the brain, Waves in Random and Complex Media, DOI: 10.1080/17455030.2021.1938746

To link to this article: https://doi.org/10.1080/17455030.2021.1938746

Published online: 10 Jun 2021.

WAVES IN RANDOM AND COMPLEX MEDIA
https://doi.org/10.1080/17455030.2021.1938746

Taylor & Francis
Taylor & Francis Group

A neuronal population model based on cellular automata to simulate the electrical waves of the brain

Ali Khaleghi[a], Mohammad Reza Mohammadi[a], Kian Shahi[a] and Ali Motie Nasrabadi[b]

[a]Psychiatry and Psychology Research Center, Tehran University of Medical Sciences, Tehran, Iran; [b]Biomedical Engineering Department, Shahed University, Tehran, Iran

ABSTRACT

Neural oscillations as synchronized activity of large numbers of neurons in the neural ensembles have always been a hot topic of research for experimental and theoretical studies because of their high importance in human behaviors and functions. Since there is not yet a comprehensive mathematical model for simulating brainwaves, we proposed a cellular automaton (CA) model of a neuronal population by considering the different states of an action potential at the cellular level and simple connectivity patterns . Some important characteristics of a neural network are included in the model, such as different states of activation of a neuron, and excitatory and inhibitory synapses. Our computational model can display different dynamics from fixed-point and limit-cycle to chaotic behaviors similar to different dynamics of a real neuronal population in the brain. Qualitative and quantitative comparisons of the real electroencephalogram data and the CA simulations in the linear and nonlinear domains demonstrated the efficiency of our CA network to simulate the electrical brain activity. Time series from the proposed model display a high-dimensional stochastic behavior that corresponds to the behavior of a healthy brain. Therefore, this model can be used to study biological neuronal populations and provide more insight into their different mechanisms.

ARTICLE HISTORY
Received 23 September 2020
Accepted 31 May 2021

KEYWORDS
Simulation; cellular automata; neuronal population; nonlinear dynamics; brain waves

Introduction

The human brain and nervous system is a very attractive biological system because of its highly complex structure and its subtle function. Multilayer structures with different levels on spatial scales, from molecular to the whole population, form the basis of biological mechanisms in the nervous system. A neuron is an important component in the nervous system that is responsible for signal processing. Neurons are able to produce electrical potentials, under external conditions, that are used to send information to other cells that are connected to them. They use cascades of biological reactions for information processing in the nervous system. Individual neurons are not the whole story. They connect and compose neuronal populations and networks. A small number of reciprocally connected neurons can produce complex behaviors and have information processing

CONTACT Ali Khaleghi alikhaleghi_bme84@yahoo.com

capabilities that do not exist in a single neuron. However, the complexity of neuronal populations makes it difficult to theorize about how such neurons interact and how they function. This makes computational studies essential and important for the development, verification and validation of hypotheses. In fact, understanding networks of interacting neurons and their mechanisms is the main domain in computational and theoretical neuroscience. Mathematical modeling of biological systems is a classical subject of theoretical and computational biology to understand, test and interpret biological phenomena. Mathematical models of the collective activity of neuronal populations can be very important to understand the large-scale neuroimaging data and to get more insight into cognitive neuroscience. Therefore, mathematical modeling has become an attractive branch of neuroscience and a tool for neuroscientists to investigate the behaviors of neuronal populations at different scales [1–6].

In recent decades, various tools and methods such as artificial neural networks (ANNs) have been developed that have had various applications in mathematical biomodeling and computational neuroscience such as electroencephalogram (EEG) simulation. However, serious limitations such as numerous parameters, high computational costs, and lack of transparency of neural mechanisms have led to the limitation of some methods such as ANNs, nonlinear ordinary differential equations, and Hodgkin–Huxley-based models. Cellular automata (CA) as an advanced engineering tool offer us good flexibility in modeling the function of neurons. CA is a mathematical approach to model real systems with numerous agents working together and generating global patterns of behavior. CA provides a theoretical framework in which a set of many interactive cells connect to each other based on established interaction rules in time and space. Then, CA behavior is determined based on the number of cells, their dynamic properties and their interactions with each other [7]. Today, different versions of the CA such as continuous CA, probabilistic CA and CA with dynamic rules have been used in the field of neuroscience and yielded promising findings for the explanation of some cognitive functions of the brain [7,8]. As shown in previous studies [9–11], the dynamic properties of CA make it a suitable tool for modeling different types of neuronal activities. For instance, Beigzadeh and Hashemi [12] proposed a phenomenological CA based model of the visual cortex. Acedo et al. [13] have also simulated normal and abnormal EEG by a large number of automata and high density connections between them. Compared to other computational methods such as artificial neural networks, globally coupled maps and coupled neural networks, CA enables us to define the behavior of cells and their connectivity patterns locally and globally [7,11].

Although it is possible to introduce physiological details at the cellular level in a CA model with minimal computational costs, previous studies have paid less attention to such details. In this study, we intend to model a neuronal population by considering the different states of an action potential at the cellular level and simple connectivity patterns. For this purpose, we use simple rules with minimal parameters to achieve high generalizability and low computational volume. We hypothesize that such a simple network will be able to produce a variety of dynamic behaviors, and will also be able to exhibit dynamical properties similar to the inherent properties of a real neuronal population in the brain. Therefore, we will compare the output waves from the CA network with the electrical waves of the cerebral cortex (i.e. EEG signal).

Methods and materials

Proposed model

CA is a nonlinear, discrete and spatiotemporal method, which is comprised of many simple components capable of complex behaviors when working together. In fact, CA consists of a set of cells interacting according to some rules. Each cell has a set of states and a neighborhood. Therefore, CA is defined based on four basic concepts including a lattice of sites, states, neighborhoods, and rules [7]. In this section, we explain the mathematical framework, different parameters, rules and details of the model. This model was implemented using the Python language. The steps for the operation of the proposed CA algorithm is as follows:

(1) Start algorithm,
(2) Define a two-dimensional lattice N $\times$ N,
(3) Define the initial conditions for cells through a random number generator based on different phases of an action potential,

$$S = \Phi_{AP}.\begin{cases} AP = 0 \quad \textit{resting state} \\ AP = 1.2.3.4 \quad \textit{firing state} \\ AP = 5 \quad \textit{hyperpolarization state} \\ AP = 6.7.8.9.10 \quad \textit{refractory state} \end{cases}$$

(4) Define the active number of synapses or neighborhoods that each cell can have, as $N_{\min}$ to $N_{\max}$ where $N_{\max} < N$,
(5) Apply the following rules that each cell obeys:
   (a) A resting neuron is activated when the sum of synapses inputs from the neighbor cells exceeds a resting threshold T_{rest}.

$$P(t.i.j) : \begin{cases} \Phi_{AP} = \Phi_{AP+1}.\text{if} C_e - C_i - \alpha C_h \geq T_{rest} \\ \Phi_{AP} = \Phi_{AP}.\text{if} C_e - C_i - \alpha C_h < T_{rest} \end{cases} .AP = 0.1.\ldots.10$$

where $P(t,i,j)$ indicates the state of a neuron in position (i,j) and at time t based on the specified phases of an action potential; C_e, C_i and C_h indicate the number of excitatory neighbor neurons, inhibitory neighbor neurons and neighbor neurons in hyperpolarization state, respectively; and α is the hyperpolarization coefficient.

   (b) After activation, a neuron must pass firing, hyperpolarization and refractory states and then return to the resting state.
   (c) In a hyperpolarization state, the neuron cannot generate a subsequent action potential.
   (d) In the firing state, a neuron can never be activated again by its neighbors at all. But in the refractory period, a neuron can be activated again when the stimulation from its neighbors reaches T_{relative} ($T_{\text{relative}} > T_{\text{rest}}$).

$$P(t.i.j) : \begin{cases} \Phi_{AP} = \Phi_{AP+1}.\text{if} C_e - C_i - \alpha C_h \geq T_{\text{relative}} \\ \Phi_{AP} = \Phi_{AP}.\text{if} C_e - C_i - \alpha C_h < T_{\text{relative}} \end{cases} .AP = 0.1.\ldots.10$$

(6) Extract time series as output with the sum of the effect of each neuron.

$$y(t) = \sum_{t=0}^{n} W(P)P(t.i.j).W(P) = \{V(\Phi_0).V(\Phi_1).\ldots.V(\Phi_{10})\}$$

where $W(P)$ indicates the values of each of the specified phases of the action potential.

Real data for comparison

In addition to visual inspection, we performed various quantitative linear and nonlinear analyzes to more accurately compare the time series generated by the network and the real data. For this purpose, we used publicly available EEG data taken from Physionet [14]. The database includes 36 EEG recordings of healthy adults in the resting-state as well as when performing arithmetic tasks. Signals were recorded using a Neurocom EEG system (Ukraine, XAI-MEDICA) based on the international 10–20 protocol through Ag/AgCl electrodes with the interconnected ear reference electrodes. At the preprocessing step, a notch filter (50 Hz) and a high-pass filter with a cut-off frequency of 30 Hz were applied to all data. The independent component analysis was applied to eliminate the artifacts, and thus, an artifact-free EEG segment of 60 s duration was provided for each subject.

Linear and nonlinear analyzes for model validation

Spectral analysis

We used spectral analysis as a linear analysis of real and simulated time series to compare the frequency contents of both signals. We used the Welch method with a Hanning window to separate the frequency components of time series into six frequency bands: delta (1–4 Hz), theta (4–8 Hz), alpha (8–12 Hz), sigma (12–16 Hz), beta (16–24 Hz) and gamma (24–30 Hz). The window length was 256 samples with 128 overlapping samples. This algorithm is a Fourier based method that estimates the power spectrum density (PSD) of the time series [15].

Recurrence quantification analysis (RQA)

RQA is an approach for nonlinear data analysis that quantifies the recurrent behavior of the phase space trajectory of dynamical systems. It was developed to measure differently appearing recurrence plots (RPs) according to their small scale structures [16–18].

To quantitatively compare the structures in the RPs, we calculated several measures as follows:

Averaged diagonal line length is the mean length of the diagonal lines:

$$L = \frac{\sum_{l=l_{\min}}^{N} lh(l)}{\sum_{l=l_{\min}}^{N} h(l)}$$

where N is the number of measured points in the phase space trajectory, and $h(l)$ is the histogram of diagonal lines of length l.

The maximum diagonal line is the length of the largest diagonal line:

$$L_{\max} = (\{l_i\}; i = 1.\cdots.N_l)$$

where N_l is the number of whole diagonal lines in the RP.

Trapping time is the mean length of the vertical lines:

$$TT = \frac{\sum_{v=v_{\min}}^{N} vh(v)}{\sum_{v=v_{\min}}^{N} h(v)}$$

where $h(v)$ is the histogram of vertical lines of length v.

The maximum vertical line is the length of the largest vertical line:

$$V_{\max} = \max(\{v_i\}; i = 1.\cdots .N_v)$$

Determinism refers to the recurrence points that form diagonal lines:

$$DET = \frac{\sum_{l=l_{\min}}^{N} lh(l)}{\sum_{l=1}^{N} lh(l)}$$

RPs of chaotic time series have more structures in the diagonal lines than stochastic processes and less than deterministic ones.

Laminarity is the recurrence points that form vertical lines:

$$LAM = \frac{\sum_{v=v_{\min}}^{N} vh(v)}{\sum_{v=1}^{N} vh(v)}$$

Fractal analysis

Fractal dimension is a statistical index to characterize fractal patterns by measuring their complexity as a ratio of the detail changes to the scale changes [19,20]. There are several techniques for calculating the fractal dimension [21]. To investigate fractal patterns in real and simulated time series, we used Petrosian and Katz methods as follows.

$$FD_{\text{Petrosian}} = \frac{\log n}{\log n + \log(n/(n + 0.4N_{\Delta}))}$$

where n and N_{Δ} are the numbers of samples and sign changes in the binary time series, respectively, that is obtained from the original time series in the Petrosian algorithm.

$$FD_{\text{Katz}} = \frac{\ln(N-1)}{\ln(N-1) - \ln(d/L)}$$

where N, d and L indicate the length of sequence data, the diameter of a data sequence, and the sum of distances between sequential points, respectively. In general, the Petrosian method considers local extrema of time series to determine the fractal patterns, while the Katz method considers the amplitude differences to calculate the fractal dimension.

Entropy analysis

Entropy is an index of randomness and complexity of dynamic systems, explaining the rate of information development [22,23]. There are various algorithms for estimating the entropy of a time series representing a dynamic system [24]. The sample entropy method is a modified version of the approximate entropy that reduces the self-matching bias and

is independent of the length of the data, and also has relative consistency in different conditions.

$$SampEn(m.r.N) = -\ln(A^m(r)/B^m(r))$$

where m, r and N represent embedding dimension, tolerance and the number of data points, respectively. $B^m(r)$ indicates the probability that if two sequences of data points of length m have a distance smaller than the tolerance r, and $A^m(r)$ defines the similar probability for two sequences of data points of length $m+1$. Here, we took $m = 2$ and $r = 0.2 \times$ SD, where SD is the standard deviation of the time series. Permutation entropy is another way to quantify the complexity of a time series by mapping a continuous time series to a symbolic sequence. The normalized permutation entropy is given by

$$PE = -\frac{\sum_{i=1}^{n!} p_i \ln p_i}{\ln n!}$$

where p_i denotes the relative frequencies of the possible patterns of the symbolic sequences, called permutations. Also, n is the embedding dimension of time series or the order of permutation [25,26].

Furthermore, multiscale entropy (MSE) is an extension of the sample entropy method to evaluate the degree of complexity in physiological signals through temporal coarse-graining procedure [27]. For the calculation of MSE, the original time series is coarse-grained by the scaling parameter (τ), with nonoverlapping windows as follows:

$$y_j^{(\tau)} = \left(\frac{1}{\tau}\right) \sum_{i=(j-1)\tau+1}^{j\tau} x_i.1 \le j \le N/\tau$$

The time series $y^{(1)}$ is simply equivalent to the original one for the first scale. Then, the sample entropy is computed for each time series with various time scales. Therefore, MSE is composed of determinations of sample entropy at each scale value.

Lempel-Ziv complexity

Lempel-Ziv complexity is the last measure we used to examine and compare the nonlinear dynamics of real and simulated time series [28,29].

$$LZC = \frac{\ln(n) \cdot c(n)}{n}$$

where n denotes the samples of time series and c(n) is the number of new subsequences in a binary time series that is obtained from the original time series, often using thresholding through a median value of the time series.

Statistical analysis

Briefly, a normality test was first performed to determine the data distribution. For this purpose, the Shapiro–Wilk test was used. This test and its statistics can determine whether the data follow a normal distribution. Shapiro–Wilk test indicated that the data had a normal distribution ($P > 0.05$). therefore, we have to use parametric tests to determine the statistically significant differences between the features extracted from the real and simulated EEG

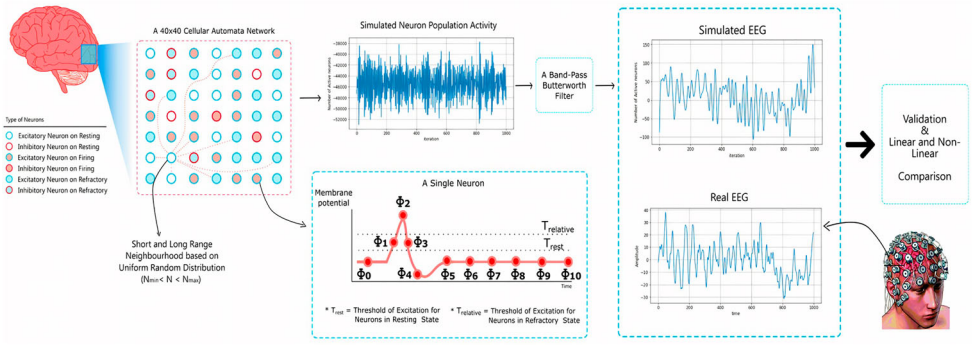

Figure 1. Schematic diagram of the proposed workflow.

signals. As a result, in this study, we used the independent t-test as a parametric statistical test to compare the means of the two groups. All statistical analyzes were conducted using SPSS (version 21) and $P < 0.05$ was considered as a significant criterion.

Results

We examined the different sizes of the neuron network and chose a 40×40 CA grid to maintain generalizability and make a compromise between computation time and efficient coding. Figure 1 shows a schematic diagram of the proposed workflow. Various experiments showed that this network is able to produce different dynamics from fixed-point and limit-cycle to highly nonlinear dynamics, yielding complex aperiodic nonlinear oscillations, depending on the values of the parameters. To get started, we had to determine the number of neurons in each resting, firing, hyperpolarization and refractory states. For this purpose, we tested different conditions and found that the dynamics of the lattice will be destroyed if either N_{rest} is greater than both N_{firing} and $N_{refractory}$, or $N_{refractory}$ is greater than N_{firing}. In other words, to maintain the dynamics of the lattice, the percentage of the resting neurons should not be larger than the neurons in the firing state and the neurons in the refractory state. Also, the percentage of neurons in the refractory state should not be larger than the neurons in the firing state. This may indicate that most of the neurons in a neuron population should be in the firing period; otherwise, the neuronal population probably will lose its function. Based on results, optimal behavior of lattice was obtained for $N_{rest} = 20\%$, $N_{firing} = 40\%$, $N_{refractory} = 35\%$ and $N_{hyperpolarization} = 5\%$. Furthermore, a fraction of cells (i.e. 20%) were labeled as inhibitory neurons and the rest (i.e. 80%) were labeled as excitatory neurons.

The results showed that the network is the most sensitive to the active number of synapses, N_{min} to N_{max}. For this reason, we set the other parameters in optimal values and examined the different states for the number of neighborhoods that each cell can have. Note that since our goal is to mimic the chaotic behavior of a neuronal population in the brain and ultimately to simulate EEG oscillations, chaotic behavior from the CA network is considered the best scenario here. Therefore, we set $T_{rest} = 8$, $T_{relative} = 12$ and $\alpha = 0.1$. Numerous conditions and values were tested for N_{min} and N_{max}, and the outputs obtained from the network were examined. In summary, experiments showed that the network yields chaotic behavior for a small range of these two parameters ($N_{min} = 14$, 15,

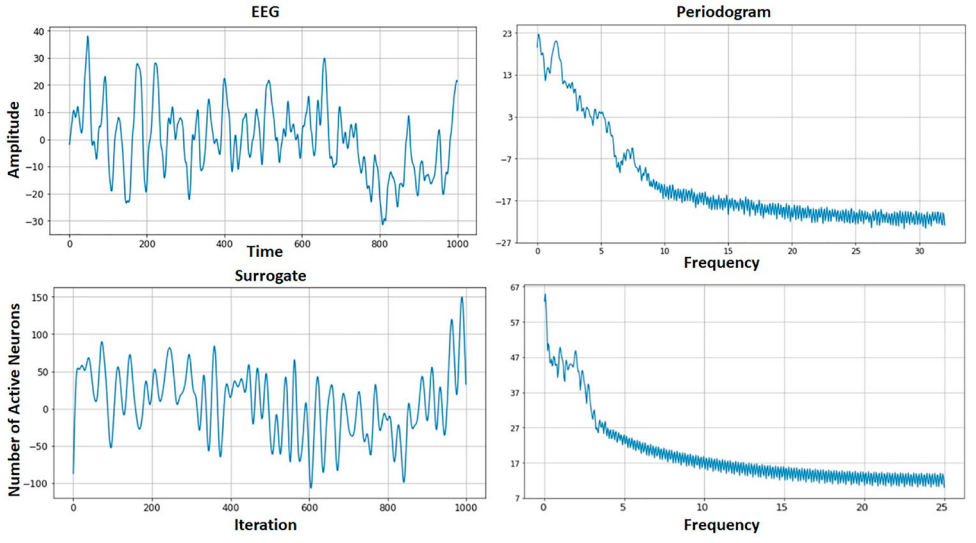

Figure 2. An example of real EEG and simulated time series produced by the cellular automata network with their periodograms. The top row indicates real EEG data and the bottom row indicates the simulated time series.

60 and $N_{max} = 60, 61, 62$), and the output time series behave similarly to EEG time series. Based on our observations, $N_{min} = 14$ and $N_{max} = 60$ were the optimal values for these two parameters. However, qualitative and quantitative analysis showed that despite the general similarity of the behavior of network output time series with brain signals, there is still a clear difference between them. For this reason, we applied a band-pass fourth-order Butterworth filter with a low cut-off frequency of 1 Hz and a high cut-off frequency of 50 Hz to the output time series of the network to consider the effects of skin, electrode, skin-electrode interface and so on during EEG recording.

Figure 2 shows an example of real EEG and simulated time series with their periodograms. As it is seen, there is a good similarity between real and simulated time series, so that both time series have strong activity in the low frequency spectrum and a weak activity in the high frequency spectrum.

In addition to visual inspection, we performed various quantitative linear and nonlinear analyzes to more accurately compare the time series generated by the network and the real data. Therefore, we ran the CA network 40 times with the above parameters and saved the generated time series for further analysis. The method of surrogate data is used in subsequent analyzes to distinguish between nonlinearity and linearity as well as between pure stochasticity and chaoticity. This method was utilized because a linear stochastic time series can imitate a nonlinear chaotic process following a static nonlinear distortion [30]. Surrogate data are created based on [31] to mimic the original data, relating to their amplitude distribution and autocorrelation.

After PSD estimation in linear analysis, relative power was calculated for each frequency band. Figure 3 shows the box plots, the receiving operating curve (ROC) and results of the statistical comparison of the relative power of the six frequency bands between the real and simulated time series. As shown in this Figure, there is no significant difference between the

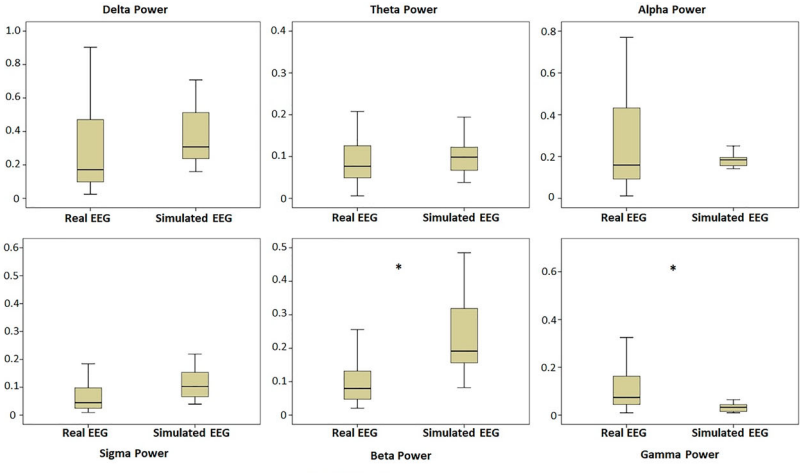

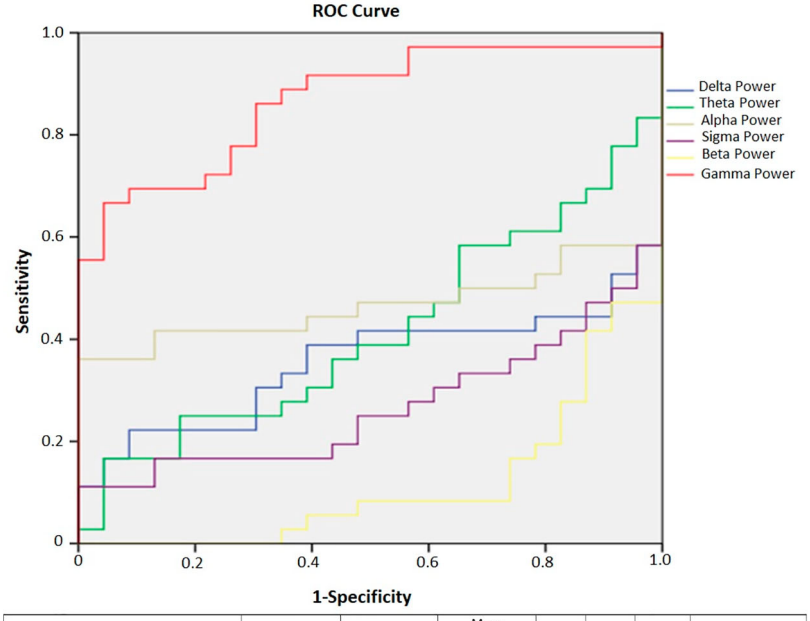

Dependent variables	Real EEG (mean±SD)	Simulated EEG (mean±SD)	Mean difference (real-simulation)	SE	t	P	95% confidence interval
Relative delta power	0.30±0.25	0.36±0.15	-0.06	0.058	-1.03	0.30	[-0.17,0.05]
Relative theta power	0.10±0.08	0.11±0.06	-0.01	0.019	-0.51	0.60	[-0.04,0.02]
Relative alpha power	0.25±0.21	0.18±0.03	0.07	0.04	1.58	0.11	[-0.01,0.11]
Relative sigma power	0.086±0.109	0.112±0.053	-0.026	0.024	-1.06	0.29	[-0.07,0.02]
Relative beta power	0.096±0.065	0.242±0.119	-0.146	0.024	-6.09	0.001*	[-0.19,-0.09]
Relative gamma power	0.012±0.013	0.003±0.001	0.009	0.003	3.30	0.001*	[0.003,0.014]

Figure 3. Box plots, ROC curve and statistical comparison of frequency components of real and simulated EEG time series in six frequency bands.

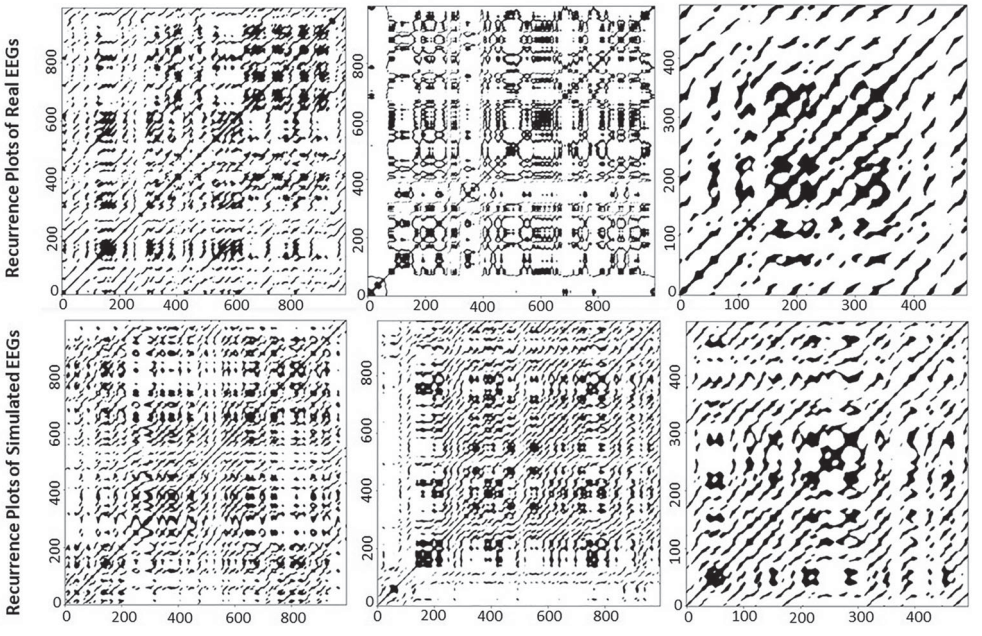

Figure 4. Examples of recurrence plots of real EEG and simulated time series produced by the cellular automata network. The top row indicates real EEG data and the bottom row indicates the simulated time series.

time series in the low frequency range (i.e. up to 16 Hz), but in the high frequency range (i.e. 16–30 Hz) there is a significant difference between them.

Moreover, as mentioned before, we used RQA, fractal and entropy analyzes to compare the nonlinear dynamics and information patterns of the real and simulated time series for model validation. Figure 4 shows examples of RPs of real and simulated time series. We can see a good similarity between the RPs of both time series. Furthermore, Figure 5 shows the box plots, ROC curve and results of the statistical comparison of the RQA features between the real and simulated time series. As shown in this Figure, only the maximum diagonal line (L_{max}) has a significant difference between the two time series and the other features reveal no significant differences between them. Figure 6 also shows the box plots, ROC curve and results of the statistical comparison of the fractal, entropy and Lempel-Ziv features between the real and simulated time series. As shown in the Figure, there are no significant differences between the two time series in terms of fractal, information and complexity patterns. Figure 7 indicates MSE curves of real and simulated EEG data. Statistical analysis revealed no significant differences between the two time series. Furthermore, Figure 8 shows the entropy values of the sub-bands and the statistical comparison of these values between the real and simulated signals; there was a significant difference between them in beta and gamma frequencies.

Discussion

CA is an important tool in statistical mechanics with a wide range of applications to complex dynamical systems. However, there have been few applications of this concept concerning

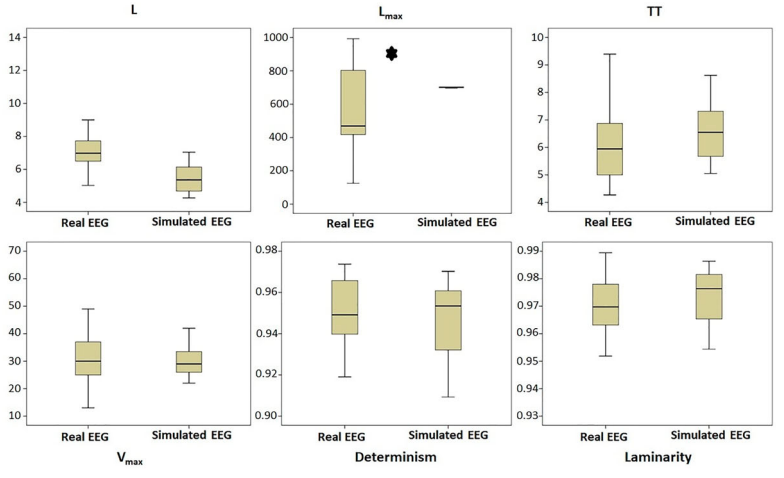

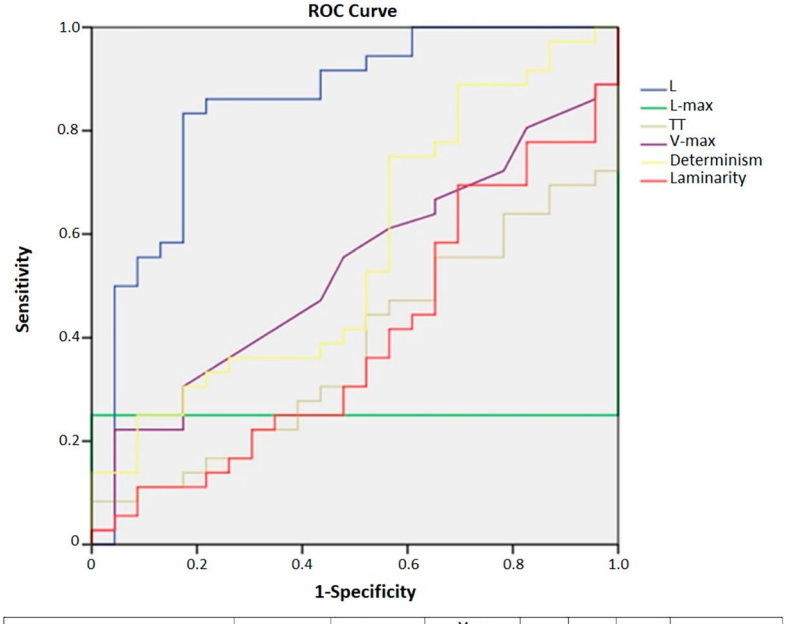

Dependent variables	Real EEG (mean±SD)	Simulated EEG (mean±SD)	Mean difference (real-simulation)	SE	t	P	95% confidence interval
Averaged diagonal line length (L)	7.14±1.27	6.51±1.92	0.63	0.41	1.51	0.13	[-0.20, 1.46]
Maximum diagonal line (L_{max})	562.02±265.92	700.52±1.70	-138.50	55.62	-2.49	0.015*	[-249.88,-27.11]
Trapping time (TT)	6.14±1.33	6.56±1.04	-0.42	0.32	-1.28	0.20	[-1.07,0.23]
Maximum vertical line (V_{max})	33.16±11.98	31.30±8.70	1.86	2.89	0.64	0.52	[-3.93,7.65]
Determinism	0.950±0.015	0.946±0.017	0.004	0.004	0.92	0.35	[-0.004,0.012]
Laminarity	0.969±0.011	0.973±0.009	-0.004	0.003	-1.38	0.17	[-0.009,0.001]

Figure 5. Box plots, ROC curve and statistical comparison of six RQA features of real and simulated EEG time series.

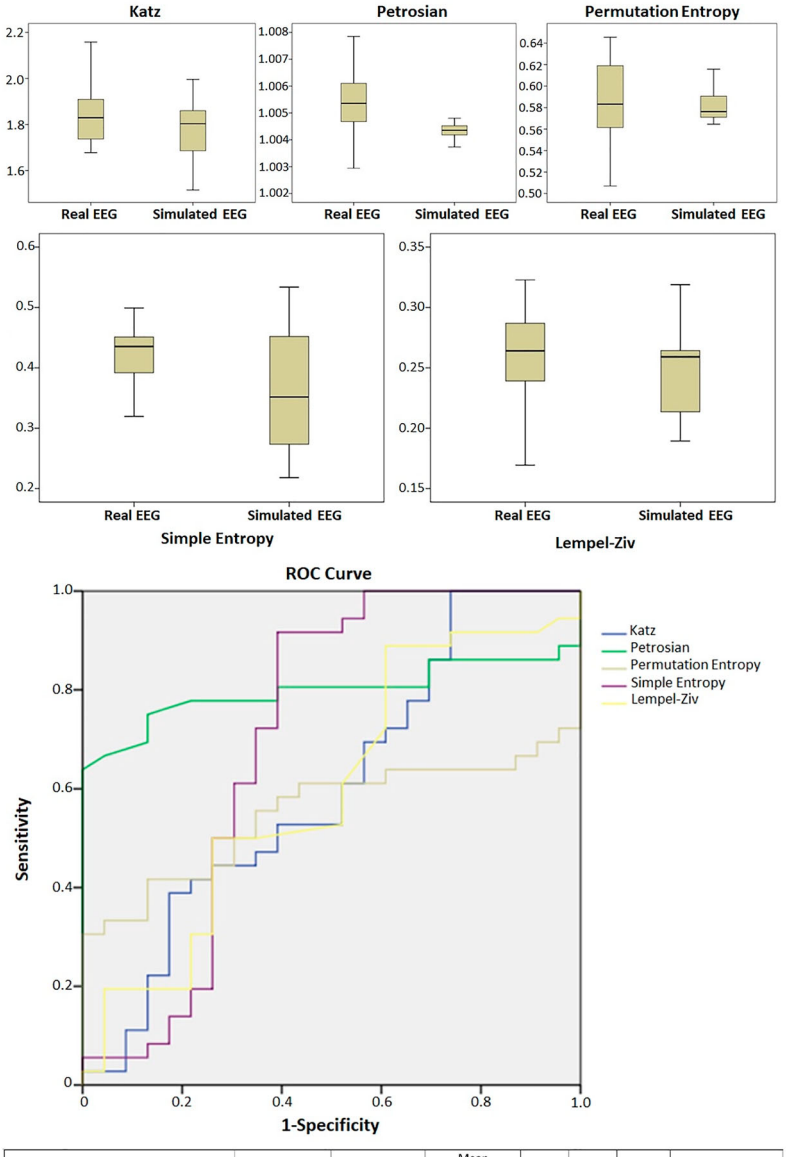

Dependent variables	Real EEG (mean±SD)	Simulated EEG (mean±SD)	Mean difference (real-simulation)	SE	t	P	95% confidence interval
Katz fractal dimension	1.84±0.11	1.79±0.15	0.05	0.03	1.47	0.14	[-0.01,0.11]
Petrosian fractal dimension	1.113±0.04	1.110±0.009	0.003	0.008	0.35	0.72	[-0.01,0.02]
Permutation entropy	0.585±0.036	0.581±0.014	0.004	0.008	0.50	0.61	[-0.011,0.019]
Sample entropy	0.42±0.05	0.39±0.10	0.03	0.02	1.53	0.13	[-0.009,0.063]
Lempel-Ziv complexity	0.260±0.035	0.247±0.036	0.013	0.009	1.37	0.17	[-0.005,0.031]

Figure 6. Box plots, ROC curve and statistical comparison of fractal, entropy and Lempel-ziv features of real and simulated EEG time series.

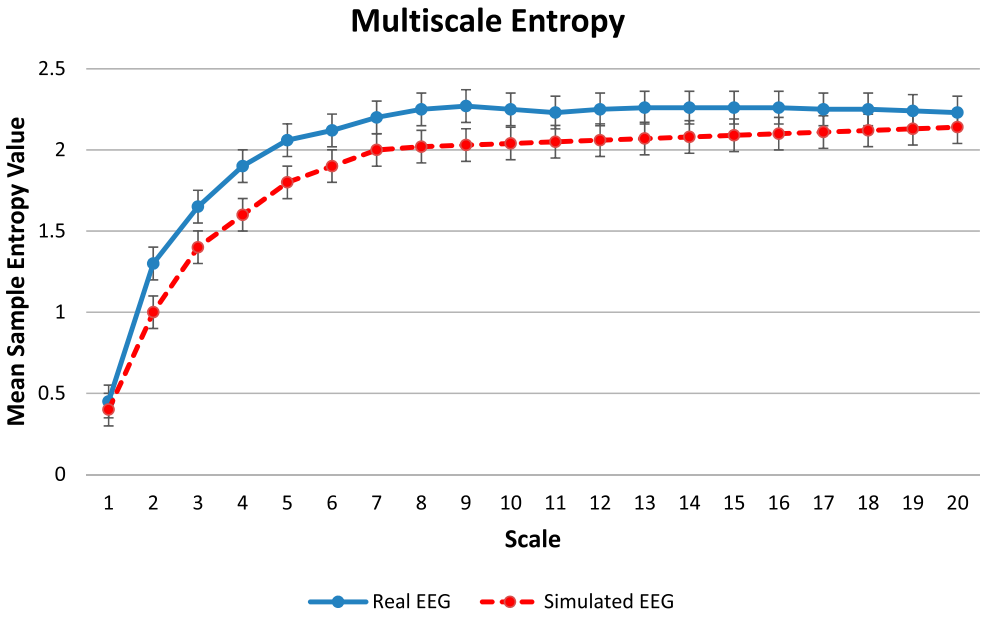

Figure 7. Mutltiscale entropy (MSE) curves of real and simulated EEG data. Statistical analysis revealed no significant differences between the two time series.

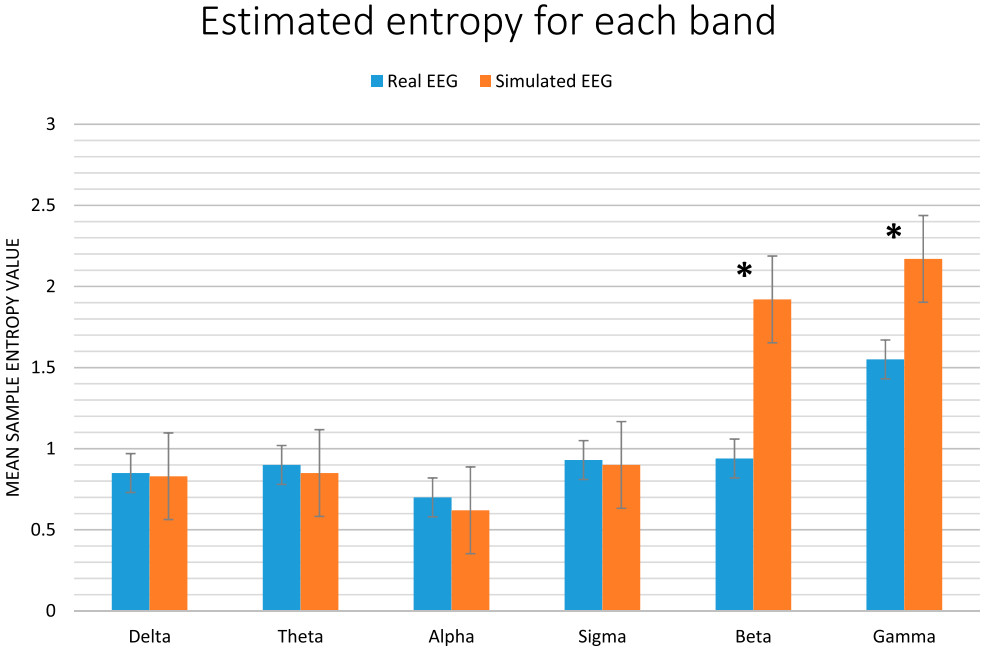

Figure 8. entropy values of the sub-bands and the statistical comparison of these values between the real and simulated signals. Asterisks indicate a significant difference ($P < 0.05$).

modelization and simulation of brain activity, as the basic example of a highly complex system. Moreover, even fewer studies have attempted to simulate electrical waves in the cerebral cortex using the CA concept, and these few studies have been conducted with

serious limitations. For instance, although the model proposed by Beigzadeh and Hashemi [12] covers some important details of a neuronal population in the visual cortex and was able to yield different dynamics with a similar frequency spectrum as the chaotic time series, their model suffers from high complexity and many parameters that must be carefully tuned with extensive efforts. The authors also did not provide an accurate nonlinear analysis for the model outputs or direct comparison with real data. In their probabilistic CA model, Acedo et al. [13] implemented a large network of neurons (10^6) based on some details of an action potential and a neuronal population in the brain. Although their model did not include many parameters, the large number of neurons led to a very high computational cost that required distributed computing. However, Goltsev et al. [32] in their study showed that small groups of 50–1000 neurons in CA networks could exhibit oscillations similar to large networks. Tsoutsouras et al. [33] implemented a simple 50×50 CA network with intra- and inter-layer connections and performed both linear and nonlinear analyzes to compare the CA simulation time series and the real EEG signals. Although they reported interesting results based on linear and nonlinear similarities of the simulated data with the real data, their model lacks important biological details of the brain neurons. They considered only the on or off states for the activity of a neuron in the network and defined all network synapses as excitatory. In fact, they greatly simplified the function of a neuron in a neuronal population. Table 1 indicates the methods and outcomes of previous studies. As shown, for the first time (to the best of our knowledge), we considered four different states to more realistically model the function of neurons and performed a quantitative statistical comparison with multiple real EEG data to validate the proposed model.

In this work, we examined the capability of the cellular automata in modeling the behavior of a neuronal population and simulating electrical waves in the cerebral cortex. For this purpose, we used new, yet simple rules for the model that would both keep the computational costs low and exhibit a realistic behavior of the neuronal population. Inspired by the action potential, we were able to model four states for each neuron including the resting, firing, refractory and hyperpolarization states. In the next step, we successfully presented the visual and statistical comparison of the real EEG data and the CA simulation data in the linear and nonlinear domains. The comparison demonstrated the efficiency of our CA network to simulate the electrical brain activity since the outputs of CA simulations were found in a good qualitative and quantitative agreement with the real data. In fact, the time series from the proposed model display a high dimensional stochastic behavior that corresponds to the behavior of a healthy brain. Our CA network was able to generate chaotic attractors and complex nonlinear oscillations. The existence of such waves in the brain signals would give clear support for the proposed model, and probably for this supposition that collective neuronal dynamics can retain the nonlinear properties of microscopic scales. However, we used surrogate data testing to make a more accurate comparison of the nonlinear dynamics of real and simulated time series.

As shown in Figure 2, both the real and simulated signals show a similar frequency and power spectrum pattern, with only a statistically significant difference between them in the high frequency components. It should be noted that in the actual recording of EEG signals, low-pass filters are frequently applied to eliminate the effect of high frequency noises, such as power line. For this reason and as mentioned, a 30-Hz low-pass filter (gamma band) has been applied to the real EEGs, and the response of this filter may have continued to lower frequencies (beta band). As a result, the existence of such a difference in the high

Table 1. Cellular automata model comparison of previous studies.

Author (year)	Method	Validation	Outcomes
Puljic et al. (2008) [10]	A two-layer probabilistic CA (lattices of size 4×4) with two bidirectional links from excitatory layer to the inhibitory one with neurons in the two states of active or inactive	Quantitative analysis on the model output without comparison with real EEG data	The model presents narrow-band oscillations when restricted to a range of inhibition levels, similar to some fluctuations in the EEG
Acedo (2009) [9]	A complete graph of N (excitatory) + M (inhibitory) Boolean automata with active and inactive states according to the Markovian evolution equations.	Quantitative analysis on the model output with a relative comparison, but not statistical comparison, with two real EEG data by mapping some model parameters to an individual's alpha and delta rhythms	Relatively good agreement between the EEG signals and CA model according to the sub-diffusive dynamics and statistical features of EEG such as the proportion between the variances of the highest amplitude signals and the lowest ones
Goltsev et al. (2010) [23]	A CA model of inhibitory and excitatory neurons with synaptic connections according to the Dale's principle	Quantitative and qualitative analysis on the model output without statistical comparison with real EEG data	The model exhibited different patterns of self-organization of neuronal networks, hysteresis, hybrid phase transitions, and a full set of dynamical phenomena caused by noise: stable and decaying fluctuations, and stochastic resonance
Tsoutsouras et al. (2012) [24]	Two 50×50 CA lattices of excitatory active and inactive neurons with both local and global connections, corresponding to the healthy and pathological areas in the limbic brain	Quantitative and qualitative analysis on the model output with some statistical comparisons (only for nonlinear dynamics) with five real EEG data	Qualitative analysis showed good consistency between simulated data and real data. Quantitative analysis was performed only on nonlinear dynamics, not on frequency spectrum, and showed the similarity of the nonlinear characteristics of the simulated data with the real data.
Kozma et al. (2013) [34]	A hierarchical neuronal network according to the concepts of random CA. Both inhibitory and excitatory active and inactive neurons with local and global neighborhoods are considered in the model	Quantitative analysis on the model output without comparison with real EEG data	The model exhibited phase transitions between limit cycle, fixed point, and broad-band chaotic regimes, also intermittent synchronization-desynchronization transitions, along with a critical region instead of a singular critical point within the cortex

(*continued*).

Table 1. Continued.

Author (year)	Method	Validation	Outcomes
Acedo et al. (2015) [13]	A CA model consisting of one million inhibitory and excitatory neurons with three firing, resting, and refractory states	Quantitative and qualitative analysis on the model output without statistical comparison with one real EEG data	Hypersynchronous waves in the mesoscopic scale that may be comparable to the real EEG recordings of patients with epilepsy in the ictal states
Beigzadeh et al. (2015) [12]	A CA model consisting of inhibitory and excitatory neuronal populations with the anatomical connectivity reported in the macaque visual cortex	Quantitative and qualitative analysis on the model output without statistical comparison with one real EEG data	The spectrum frequency of the simulated signals was similar to the spectrum of the real EEG data. Synchronization-desynchronization patterns in the simulated signals were comparable to the real patterns of the electrical activity of the brain during visual tasks.
Our model	A CA model with a size of 40×40 consisting of inhibitory and excitatory neurons with four firing, resting, hyperpolarization and refractory states, and both local and non-local connections	Quantitative and qualitative analysis on the model output with direct statistical comparison with 36 real EEG data	Statistically similar spectral pattern between the simulated signals and real EEG data, especially in lower frequency range. Statistically similar nonlinear dynamical pattern between the simulated signals and real EEG data as measured by recurrence quantification analysis, entropy methods, fractal and complexity analyzes

frequency components is not far-fetched [2,35]. In addition, it has been shown that beta and gamma frequencies arise from higher-order cognitive demand, and the synchronous activity of different cortical and subcortical networks at both resting and activated states leads to the generation of these high frequencies. However, in this work, we modeled only one neuronal population and this can cause differences observed in the power spectrum and dynamics of these two frequencies [36–39]. Although spectral analysis showed that there were differences in the power of the high frequencies, both the real data and the simulation data showed a similar spectral pattern corresponding to 1/f, which is characteristic of self-organized critical dynamical systems such as the brain [40]. In addition, we observed a phase transition in the dynamic behavior of the system by changing the minimum and maximum number of neighborhoods or cell synapses. This state on the edge (or more precisely the edge of chaos) between two different behaviors is known as the critical state, and the system in this state is at criticality [7]. Systems at criticality are considered to have capabilities of optimal memory and information processing [41]. Several theoretical neuroscience studies believe that phase transitions in the brain as a large finite system occurred not at a specific point, but are settled over a narrow region that preserves many characteristics of criticality [42]. As mentioned, this phase transition in our CA network was not limited to a point, but instead occurred for a small range of the above parameters.

The lack of significant differences between most of the features extracted from RQA analysis (5/6) indicates the fact that the mechanisms generating these two signals are similar in terms of the dynamic and chaotic structure. However, one feature (i.e. maximum diagonal line) shows a significant difference. This feature ($1/L_{\max}$) expresses the rate at which the dynamic system deviates from its original state. According to the values shown in Figure 5 for $L_{\max}$, real EEGs have a higher divergence rate than simulated signals due to the fact that in recording real EEGs from human subjects, it is practically impossible to control the subject's mental states, especially at rest. But in the computer model, the system maintains its functional state until the end of the simulation. This can well justify the significant difference between the real and simulated signals in terms of the maximum diagonal line in their RPs. The trapping time and laminarity, which indicate how change the chaotic states of the system, also confirm this issue, because both features have lower values for the real signals than the simulated ones, although the difference is not significant. Furthermore, the lack of significant differences in fractal, entropy and Lempel-Ziv features means that there is a similar pattern of nonlinear dynamics in both real and simulated time series, which somehow confirms the validity of our proposed model. However, regarding the smaller values of the features of Figure 6 for the simulated EEG, it should be noted that generally, a mathematical simulation model of a biological system cannot produce information and details as a real biological system [43–45]. Given that these features represent the structural nature and dynamic patterns of the system, their lower values for the mathematical model confirm the fact that a mathematical model, no matter how well tuned and behaves similarly to the real system, still includes less information than the real system because the real biological system has many aspects and wide variability that cannot be incorporated into a single mathematical model.

Most previous models have focused solely on one aspect of the power spectrum or nonlinear dynamics of EEG signals, while our proposed model can simulate the brain oscillatory activity as well as the nonlinear dynamics of EEG, which is confirmed by quantitative

statistical comparisons. Therefore, our model can become a suitable tool for various clinical applications. Our model, which is based on existing physiological knowledge and mathematical rules, can help to simulate and better understand the function of the brain in different conditions and can have important applications in medical research and education to examine various hypotheses about the human brain as well as in clinical and therapeutic practices to study, for example, the effects of different medications on brain function from microscopic to macroscopic levels and to predict subsequent behaviors. It is a preliminary tool to describe the basic mechanisms involved in experimentally observed behaviors in neurology, neuroscience and psychiatry at different scales, from the molecular world to that of behavior and cognition. Such a model, after appropriate scaling and optimization, can be used to study brain waves and their associated pathological mechanisms in diseases such as bipolar disorder and schizophrenia. A recent review study suggested that a combination of statistical physics with dynamical systems theory (as in our case) can provide a powerful framework and tool for modeling clinical abnormalities of the human brain [46].

Based on the observations, one of the limitations of this model is that it is suitable for modeling short-term mechanisms related to the electrical activity of the brain and is not generalizable to actual long-term activities. Adaptive selection of model parameters and consideration of a probabilistic cellular automaton model can help alleviate this limitation and increase its generalizability. In addition, validating such models is often difficult and challenging, and most previous studies have used qualitative methods to do so. However, in this study, probably for the first time, in addition to qualitative methods, we used linear and nonlinear quantitative methods and statistical analyzes to validate the proposed model, to overcome this limitation to a large extent.

Conclusion

The proposed model with five controllable parameters (the threshold for stimulating the neuron in rest, the threshold for stimulating the neuron in the refractory period, the hyperpolarization coefficient, the minimum number of neighbors of the neuron, and the maximum number of neighbors of the neuron) has the ability to display different dynamics from fixed-point and limit-cycle to chaotic behaviors. This 40×40 CA model could generate chaotic attractors and complex nonlinear oscillations similar to actual brain waves. Different linear and nonlinear analyzes including spectral, RQA, fractal, entropy and complexity analyzes proved the similarity of the simulated and real EEG signals. Therefore, this model can be used to study different biological neuronal populations and provide more insight into their different mechanisms. For instance, we can examine the mechanisms involved in various diseases such as epilepsy by changing the model parameters. Although this model showed some limitations such as the inability to model long-term neural mechanisms and memory, they can be overcome with some changes in the model parameters. In the future, other biological details such as synaptic delays can be added to the model, and by optimizing the current model, more accurate insight into the biological mechanisms involved in neural oscillations at the microscopic and macroscopic levels can be achieved.

Disclosure statement

No potential conflict of interest was reported by the author(s).

Funding

This study was funded by Tehran University of Medical Sciences and Health Services through a grant from Psychiatry and Psychology Research Center [grant number 37425].

References

[1] Bassett DS, Sporns O. Network neuroscience. Nat Neurosci. 2017;20(3):353–364.
[2] Breakspear M. Dynamic models of large-scale brain activity. Nat Neurosci. 2017;20(3):340–352.
[3] Freeman WJ. Tutorial on neurobiology: from single neurons to brain chaos. Int J Bifurcation Chaos. 1992;2(3):451–482.
[4] Izhikevich EM. Dynamical Systems in Neuroscience. The Geometry of Excitability and Bursting. Cambridge: MIT Press; 2007.
[5] Kriegeskorte N, Douglas PK. Cognitive computational neuroscience. Nat Neurosci. 2018;21(9): 1148–1160.
[6] Reeke GN, Poznanski RR, Lindsay KA, et al. Modeling in the neurosciences: from biological systems to neuromimetic robotics. Boca Raton: CRC Press; 2005.
[7] Meyers RA. Encyclopedia of complexity and systems science. New York, NY, London, UK: Springer; 2009.
[8] Beigzadeh M, Hashemi Golpayegani SMR, Gharibzadeh S. Can cellular automata be a representative model for visual perception dynamics? Front Comput Neurosci. 2013;7:130.
[9] Acedo L. A cellular automaton model for collective neural dynamics. Math Comput Model. 2009;50(5-6):717–725.
[10] Puljic M, Kozma R. Narrow-band oscillations in probabilistic cellular automata. Phys Rev E. 2008;78(2):026214.
[11] Matsubara T, Torikai H. An asynchronous recurrent network of cellular automaton-based neurons and its reproduction of spiking neural network activities. IEEE Trans Neural Netw Learn Syst. 2016;27(4):836–852.
[12] Beigzadeh AM, Hashemi GS. A cellular automaton based model for visual perception based on anatomical connections. 2015.
[13] Acedo L, Lamprianidou E, Moraño J-A, et al. Firing patterns in a random network cellular automata model of the brain. Physica A. 2015;435:111–119.
[14] Goldberger AL, Amaral LA, Glass L, et al. Physiobank, PhysioToolkit, and PhysioNet: components of a new research resource for complex physiologic signals. Circulation. 2000;101(23):e215–e220.
[15] Khaleghi A, Sheikhani A, Mohammadi MR, et al. EEG classification of adolescents with type I and type II of bipolar disorder. Australas Phys Eng Sci Med. 2015;38(4):551–559.
[16] Mehrnam A, Nasrabadi A, Ghodousi M, et al. A new approach to analyze data from EEG-based concealed face recognition system. Int J Psychophysiol. 2017;116:1–8.
[17] Ramdani S, Boyer A, Caron S, et al. Parametric recurrence quantification analysis of autoregressive processes for pattern recognition in multichannel electroencephalographic data. Pattern Recognit. 2021;109:107572.
[18] Lopes MA, Zhang J, Krzemiński D, et al. Recurrence quantification analysis of dynamic brain networks. Eur J Neurosci. 2021;53(4):1040–1059.
[19] Khaleghi A, Birgani PM, Fooladi MF, et al. Applicable features of electroencephalogram for ADHD diagnosis. Res Biomed Eng. 2020;36(1):1–11.
[20] Zakharov A, Chaplygin S, editors. Fractal analysis of EEG signals for identification of sleep-wake transition. Proceedings of the Computational Methods in Systems and Software; 2020: Springer.
[21] Wen T, Cheong KH. Invited review: the fractal dimension of complex networks: a review. Information Fusion. 2021.
[22] Mohammadi MR, Khaleghi A, Nasrabadi AM, et al. EEG classification of ADHD and normal children using non-linear features and neural network. Biomed Eng Lett. 2016;6(2):66–73.
[23] Li X, Ouyang G, Richards DA. Predictability analysis of absence seizures with permutation entropy. Epilepsy Res. 2007;77(1):70–74.

[24] Hussain L, Shah SA, Aziz W, et al. Analyzing the dynamics of sleep electroencephalographic (EEG) signals with different pathologies using threshold-dependent symbolic entropy. Waves Random Complex Media. 2020;1:1–18.
[25] Hussain L, Aziz W, Saeed S, et al. Complexity analysis of EEG motor movement with eye open and close subjects using multiscale permutation entropy (MPE) technique. 2017.
[26] Hussain L, Aziz W, Saeed S, et al. Quantifying the dynamics of electroencephalographic (EEG) signals to distinguish alcoholic and non-alcoholic subjects using an MSE based Kd tree algorithm. Biomed Eng. 2018;63(4):481–490.
[27] Hussain L, Aziz W, Alshdadi AA, et al. Multiscaled entropy analysis to quantify the dynamics of motor movement signals with fist or feet movement using topographic maps. Technol Health Care. 2020;28(3):1–15.
[28] Zarafshan H, Khaleghi A, Mohammadi MR, et al. Electroencephalogram complexity analysis in children with attention-deficit/hyperactivity disorder during a visual cognitive task. J Clin Exp Neuropsychol. 2016;38(3):361–369.
[29] Yakovleva TV, Kutepov IE, Karas AY, et al. EEG analysis in structural focal epilepsy using the methods of nonlinear dynamics (Lyapunov exponents, Lempel–Ziv complexity, and multiscale entropy). Scientific World J. 2020;2020:1–13.
[30] Theiler J, Eubank S, Longtin A, et al. Testing for nonlinearity in time series: the method of surrogate data. Physica D. 1992;58(1-4):77–94.
[31] Schreiber T, Schmitz A. Improved surrogate data for nonlinearity tests. Phys Rev Lett. 1996;77(4):635–638.
[32] Goltsev A, De Abreu F, Dorogovtsev S, et al. Stochastic cellular automata model of neural networks. Phys Rev E. 2010;81(6):061921.
[33] Tsoutsouras V, Sirakoulis GC, Pavlos GP, et al. Simulation of healthy and epileptiform brain activity using cellular automata. Int J Bifurcation Chaos. 2012;22(09):1250229.
[34] Kozma R, Puljic M. Hierarchical random cellular neural networks for system-level brain-like signal processing. Neural Netw. 2013;45:101–110.
[35] Nunez PL, Srinivasan R. A theoretical basis for standing and traveling brain waves measured with human EEG with implications for an integrated consciousness. Clin Neurophysiol. 2006;117(11):2424–2435.
[36] Kuzovkin I, Vicente R, Petton M, et al. Activations of deep convolutional neural networks are aligned with gamma band activity of human visual cortex. Commun Biol. 2018;1(1):1–12.
[37] Chen G, Zhang Y, Li X, et al. Distinct inhibitory circuits orchestrate cortical beta and gamma band oscillations. Neuron. 2017;96(6):1403–1418.e6.
[38] Mably AJ, Colgin LL. Gamma oscillations in cognitive disorders. Curr Opin Neurobiol. 2018;52:182–187.
[39] Vidaurre D, Hunt LT, Quinn AJ, et al. Spontaneous cortical activity transiently organises into frequency specific phase-coupling networks. Nat Commun. 2018;9(1):1–13.
[40] Pavlos G, Tsoutsouras V, Iliopoulos L, et al. Self organized criticality (SOC) and chaos behavior in the brain activity. Order Chaos Nonlinear Dyn Syst. 2008;10:145–155.
[41] Legenstein R, Maass W. What makes a dynamical system computationally powerful. New directions in statistical signal processing: From systems to brain. 2007:127–154.
[42] Moretti P, Muñoz MA. Griffiths phases and the stretching of criticality in brain networks. Nat Commun. 2013;4(1):1–10.
[43] Dayan P, Abbott LF. Theoretical neuroscience: computational and mathematical modeling of neural systems. Computational Neuroscience Series. 2001.
[44] Jaeger D, Jung R. Encyclopedia of computational neuroscience. New York, NY: Springer Publishing Company, Incorporated; 2015.
[45] Trappenberg T. Fundamentals of computational neuroscience. Oxford: OUP Oxford; 2009.
[46] Roberts JA, Friston KJ, Breakspear M. Clinical applications of stochastic dynamic models of the brain, part II: a review. Biol Psychiatry Cogn Neurosci Neuroimaging. 2017;2(3):225–234.